Crystal structure of *Trypanosoma cruzi* trypanothione reductase in complex with trypanothione, and the structure-based discovery of new natural product inhibitors

Charles S Bond[1†], Yihong Zhang[1‡], Matthew Berriman[2], Mark L Cunningham[3§], Alan H Fairlamb[2] and William N Hunter[2*]

Background: Trypanothione reductase (TR) helps to maintain an intracellular reducing environment in trypanosomatids, a group of protozoan parasites that afflict humans and livestock in tropical areas. This protective function is achieved via reduction of polyamine–glutathione conjugates, in particular trypanothione. TR has been validated as a chemotherapeutic target by molecular genetics methods. To assist the development of new therapeutics, we have characterised the structure of TR from the pathogen *Trypanosoma cruzi* complexed with the substrate trypanothione and have used the structure to guide database searches and molecular modelling studies.

Results: The TR–trypanothione-disulfide structure has been determined to 2.4 Å resolution. The chemical interactions involved in enzyme recognition and binding of substrate can be inferred from this structure. Comparisons with the related mammalian enzyme, glutathione reductase, explain why each enzyme is so specific for its own substrate. A CH•••O hydrogen bond can occur between the active-site histidine and a carbonyl of the substrate. This interaction contributes to enzyme specificity and mechanism by producing an electronic induced fit when substrate binds. Database searches and molecular modelling using the substrate as a template and the active site as receptor have identified a class of cyclic-polyamine natural products that are novel TR inhibitors.

Conclusions: The structure of the TR–trypanothione enzyme–substrate complex provides details of a potentially valuable drug target. This information has helped to identify a new class of enzyme inhibitors as novel lead compounds worthy of further development in the search for improved medicines to treat a range of parasitic infections.

Addresses: [1]Department of Chemistry, University of Manchester, Oxford Road, Manchester, M13 9PL, UK, [2]The Wellcome Trust Building, Department of Biochemistry, University of Dundee, Dundee, DD1 5EH, UK and [3]The London School of Hygiene and Tropical Medicine, Keppel Street, London, WC1E 7HT, UK.

Present addresses: [†]Department of Biochemistry, University of Sydney, Sydney, NSW, 2006, Australia, [‡]Laboratory of Structural Biology, National Institutes of Health, 12441 Parklawn Drive, Rockville, MD 20852, USA and [§]Department of Molecular Microbiology, Washington University School of Medicine, St. Louis, MO 63110-1093, USA.

*Corresponding author.
E-mail: w.n.hunter@dundee.ac.uk

Key words: cadabacine, Chagas' disease, lunarine, oxidoreductase, trypanothione reductase

Received: **4 September 1998**
Revisions requested: **29 October 1998**
Revisions received: **9 November 1998**
Accepted: **10 November 1998**

Published: **4 January 1999**

Structure January 1999, **7**:81–89
http://biomednet.com/elecref/096921260070081

Introduction

Protozoa belonging to the order Kinetoplastida, suborder Trypanosomatina, are the causal agents of a variety of tropical diseases that pose an important medical and economic problem for millions of people. Chagas' disease, caused by infection with *Trypanosoma cruzi*, is a particular problem in South and Central America [1]. There are no appropriate vaccines and the current therapies for trypanosomal infection are inadequate because of the low efficacy and high toxicity of the available drugs. The problem is compounded by the ability of the parasites to develop drug resistance — hence the urgent search for new and improved anti-trypanosomal agents [2]. One way forward is structure-based drug development [3,4]. In this approach a valid biochemical target, an enzyme or a metabolic pathway, is identified and characterised with respect to structure and function. The molecular detail is then used to support a search for enzyme inhibitors or protein ligands. Trypanothione reductase (TR) represents one such target for anti-trypanosomal drug development and an understanding of the enzyme is necessary to facilitate a search for inhibitors with the desired pharmacological properties.

Living cells rely on two classes of low molecular mass chemicals, polyamines and thiol-containing compounds, in a wide range of biological functions. Amongst others, polyamines are implicated in protein synthesis, cell growth and development [5], whereas the peptide glutathione (L-γ-glutamyl-L-cysteinylglycine; Figure 1a) is involved in maintaining redox balance and regulating diverse aspects of metabolism [6]. The thiol form of glutathione, GSH, functions as a protective agent, maintaining an intracellular reducing environment. GSH is oxidised to glutathione disulfide (GSSG) following reaction with potentially damaging radicals and oxidants. The enzyme glutathione reductase (GR) ensures that high thiol levels are preserved by

Figure 1

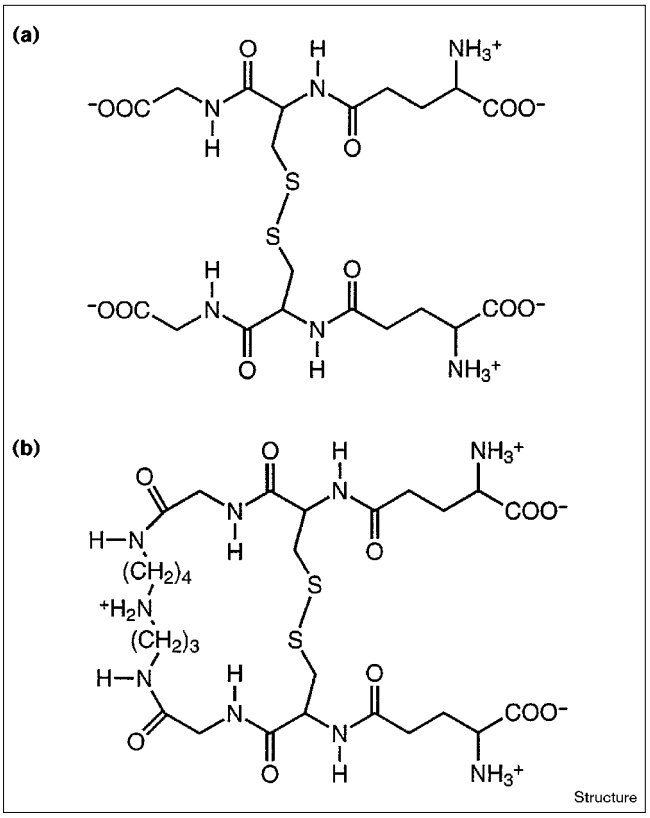

Molecular formulae for human and trypanosomal metabolites: **(a)** glutathione disulfide (GSSG) and **(b)** trypanothione disulfide ($T[S]_2$). Trypanothione comprises γGlu–Cys–Gly–Spm–Gly–Cys–γGlu with the suffix I or II to identify separate components and to be consistent with the nomenclature used previously on GSSG complexed with human GR [8]. Following reduction by the cognate enzyme, GSSG is converted to two molecules of the thiol, GSH, whereas $T[S]_2$ is converted to a single molecule of the dithiol, $T[SH]_2$.

catalysing the reduction of the disulfide. The GR–GSSG system has been thoroughly investigated by a variety of techniques, including crystallography [7].

Trypanosomatids use polyamine-glutathione adducts, instead of GSH, to function in similar protective and regulatory roles [8]. Three adducts have been identified so far: trypanothione (N^1,N^8-*bis*(glutathionyl)spermidine; Figure 1b), glutathionylspermidine and homotrypanothione [8]. Similarities with glutathione suggested that these metabolites might have a similar biological function in scavenging free radicals and oxygen-reactive species formed by metabolic processes or when the parasites are subjected to oxidative stress by the host immune response. The adducts can also regulate polyamine levels and thereby influence cell growth and development. Trypanosomes contain low levels of glutathione but do not possess GR. The enzyme trypanothione reductase is responsible for the conversion of trypanothione disulfide ($T[S]_2$) to the di-thiol form, dihydrotrypanothione ($T[SH]_2$). The di-thiol form can reduce GSSG to GSH by thiol–disulfide exchange [8]. Human GR and TR are both NADPH-dependent, flavin-containing disulfide oxidoreductases. They function as homodimers of subunit molecular mass in the range 52–54 kDa and share about 30% sequence identity. The key residues involved in catalysis are conserved but the critical observation has been made that each enzyme is specific for its cognate substrate, despite mechanistic and structural similarities [8,9]. This indicates that it should be possible to inhibit the parasite TR but not the human host GR. Furthermore, molecular genetic studies indicate that TR is essential for growth and survival of the parasites [10–12]. This validates TR and trypanothione metabolism as a target for structure-based drug design against trypanosomatids; one of only a few systems where such validation has been achieved. A complete understanding of the structure and reactivity of TR is required to support such an approach.

Previous studies provided clues about the roles of various amino acids with respect to enzyme specificity [3,7,13]. The early crystallographic research used TR from the non-pathogenic *Crithidia fasciculata* [14–16]. We decided to concentrate on *T. cruzi* TR because it represents the direct target for which new chemotherapeutic agents are sought, and therefore determined the structure at 2.3 Å resolution [17]. We now report the structure of TR in complex with the physiological substrate $T[S]_2$. This structure provides, for the first time, direct evidence of how the target enzyme interacts with this physiological substrate and explains why TR and GR are specific for their own substrates. Comparisons of disulfide oxidoreductases and serine proteases suggest that these two types of enzyme share similarities in their mechanism. The determination of the $T[S]_2$ conformation in the TR active site provides molecular templates to direct the identification of enzyme inhibitors by combining database searches and molecular modelling methods. Our successful utilisation of the structure in this way has lead to the discovery of a novel class of enzyme inhibitors.

Results and discussion

Structure of TR and location of the active site

The architecture of the TR dimer, the location of cofactor-binding domains and the substrate-binding sites are presented in Figure 2. Each subunit comprises an FAD-binding domain, an NADPH-binding domain and an interface domain, the latter of which is responsible for the assembly of the homodimer. The disulfide-substrate-binding site is ~15 Å wide and deep, 20 Å in length and is formed by residues from the FAD-binding domain and the interface domain of the partner subunit. This cleft is created by residues 15–22, 53–62, 103–114 and 335–343 from one subunit and 396′–399′ and 461′–470′ from the other (where ′ indicates a residue from the partner subunit). The residues involved in catalysis, the redox-active disulfides (Cys53 and

Figure 2

Organisation of the *T. cruzi* TR dimer. FAD and $T[S]_2$ molecules are shown as van der Waals spheres, coloured dark blue and cyan, respectively. The three distinct domains from each subunit are coloured differently: the FAD-binding domain (domain I) is in yellow; the NADPH-binding domain (domain II) is in green; and the interface domain is in red. The dimer interface is indicated by a pink line, and an arrow points to the disulphide-substrate-binding site. This figure was composed using MOLSCRIPT [36] and Raster3D [37].

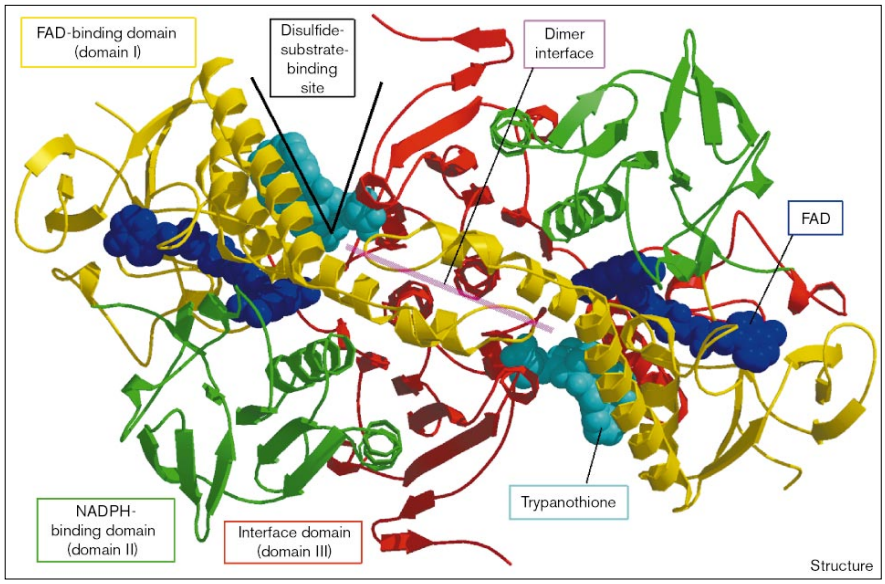

Cys58) and active-site base (His461′) are located at the bottom of the cleft near the isoalloxazine ring of FAD. As noted previously [14,17], the disulfide-substrate-binding site is one of the most ordered parts of the structure, as indicated by thermal parameters and real-space residuals. There are no large conformational changes upon binding $T[S]_2$. A least-squares fit of the native structure with the protein atoms of the enzyme–substrate complex provides root mean square (rms) deviations of 0.7 Å for all atoms and 0.25 Å for Cα atoms.

Trypanothione binding

$T[S]_2$ binds asymmetrically in the rigid TR active site (Figures 3 and 4a). One γGlu–Cys–Gly component (I) is close to the redox-active disulfides and His461′, residues that form the catalytic machinery. This segment of the substrate adopts a U shape, whereas the other tripeptide moiety, component (II), adopts an extended conformation. There are 25 amino acid residues implicated in binding $T[S]_2$ by hydrogen bonding and/or van der Waals interactions (Figure 4, Table 1). Direct enzyme–substrate hydrogen bonds involve the functional groups on side-chains of Glu19 and Tyr111 and the peptide link between the GlyI and spermidine (Spm) components. A solvent-mediated link between GlyI N with Ser15 is also apparent, as is a CH•••O hydrogen bond between His461′ Cε1 and γGluII Oδ (Figure 4a). This latter interaction will be discussed later.

The Spm bridge of $T[S]_2$ is asymmetric and the resolution of our structure does not enable a clear identification of the N^4-secondary amino group. There are no direct electrostatic interactions between the charged N^4-secondary amine group of $T[S]_2$ with the enzyme, irrespective of where we assign N^4, so an arbitrary choice was made. Binding of this part of the substrate is mediated by van der Waals and cation-π interactions, with components of a hydrophobic patch in the TR active site comprising the sidechains of Leu18, Trp22, Tyr111 and Met114. In the complex formed between *C. fasciculata* TR and glutathionylspermidine disulfide a hydrogen bond can occur between Sδ of Met113 with a terminal amino group of the ligand [14]. This interaction is not possible with $T[S]_2$ because the cyclic nature of this substrate keeps the amino group of the Spm bridge away from the corresponding residue in *T. cruzi* TR, namely Met114. Nevertheless, Met114 is an important residue as it contributes to the hydrophobic patch on one side of the active site. Solvent-accessible areas have been calculated for the $T[S]_2$ molecules in isolation and when complexed to provide an estimate of the molecular surface area involved in binding to the enzyme. This indicates that 87% of the substrate becomes buried when the complex is formed. The average area lost is about 850 $Å^2$, which in energy terms is significant and approximates to a hydrophobicity component of binding of 85 kJ mol^{-1} [14].

The human GR–GSSG complex

To fully exploit the differences between TR and GR for inhibitor design or discovery we need to understand the molecular basis for the mutually exclusive substrate specificities. It is necessary to review what is known about the GR–GSSG structure [8] (PDB entry 1GRA). GSSG in the active site of human GR and the hydrogen bonds formed between the substrate and enzyme are shown in Figure 4b. The γGlu–Cys–Gly (I) component binds at the catalytic machinery in a V shape, whereas the other tripeptide adopts

Figure 3

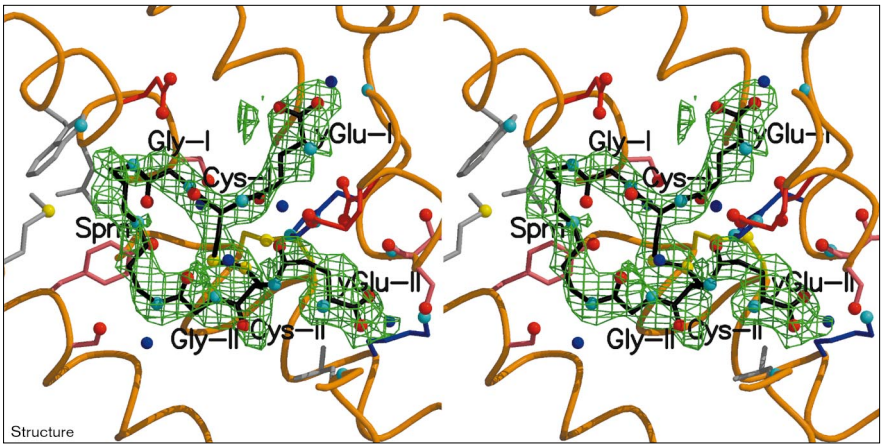

Stereoview of the omit F_{obs}–F_{calc} difference density maps for $T[S]_2$ in an active site of *T. cruzi* TR. The map (green) is contoured at a 1.5σ level. $T[S]_2$ atomic positions are shown coloured according to atom type: C, black; N, cyan; O, red; S, yellow. Solvent positions are represented by blue spheres. This figure was produced using MOLSCRIPT [36].

an extended conformation. A similar asymmetry is observed for $T[S]_2$ in the active site of TR, as discussed above. A prominent feature of the active site of human GR is a cluster of arginines: Arg37, Arg38 and Arg347, which creates a positively charged GR active site to bind the negatively charged GSSG. The enzyme–substrate interactions are dominated by hydrogen bonds formed between the side-chains of GR and GSSG. Of particular importance are the

Figure 4

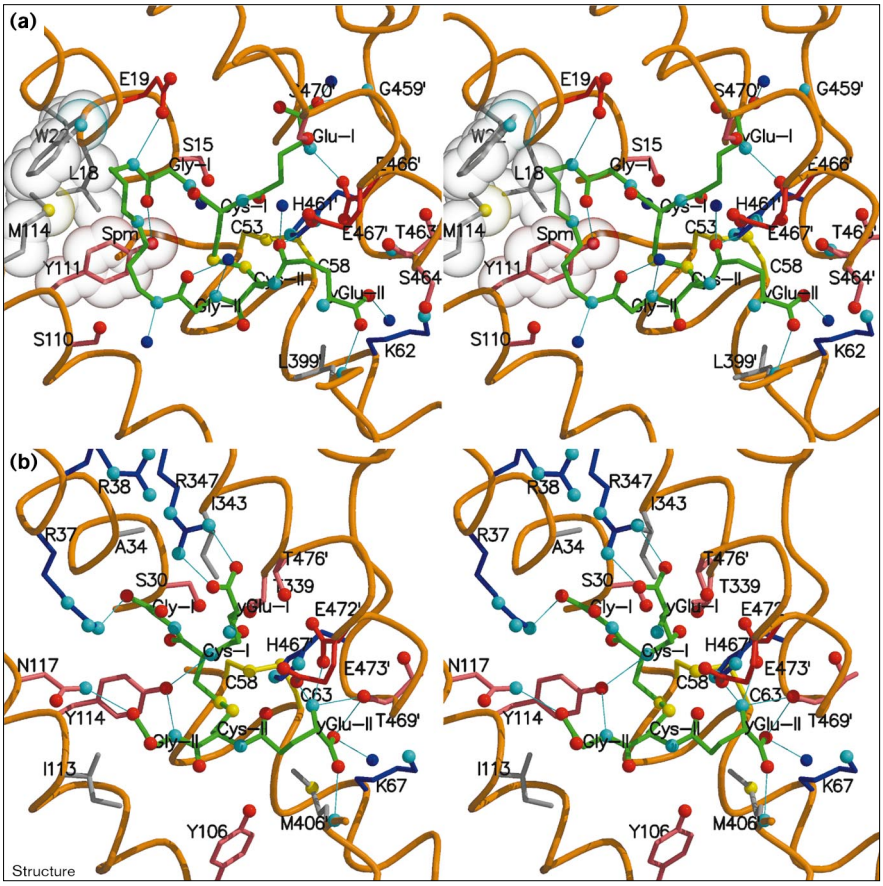

Comparison of enzyme–substrate interactions. **(a)** Stereoview of the active site of TR with bound $T[S]_2$. Selected residues are shown, labelled with the single-letter code, and sidechains are coloured according to their chemistry: basic residues are blue, acidic residues red, polar residues pink and hydrophobic residues grey. A similar atom-colouring scheme to that of Figure 3 is adopted, except that C atoms are green. Hydrogen bonds are depicted as thin continuous lines. Van der Waals surfaces are shown for residues that create a hydrophobic patch. Asn23 and Ala344 are discussed in the text but omitted from the figure because they do not interact with $T[S]_2$.
(b) Stereoview of GSSG in the active site of human GR. Solvent molecules have been removed for the sake of clarity. This figure was produced using MOLSCRIPT [36].

strong electrostatic interactions formed between the arginines at positions 37 and 347 with the GSSG carboxylates of GlyI and γGluI, respectively. Another important interaction involves the sidechain of Asn117 and the carboxylate of GlyII. In the PDB file this sidechain is positioned with Oδ1 close to a carboxylate oxygen of GlyII and in the original publication [8] this residue was described as participating in a solvent-mediated hydrogen-bonding interaction with the GlyII carboxylate. The solvent molecule also linked this carboxylate with the guanidinium of Arg37. Our assessment of the PDB entry is that a switch of the oxygen and nitrogen sidechain atoms of Asn117 would produce a direct hydrogen bond between Nδ2 and GlyII O32 of distance 3.1Å and this is what we depict in Figure 4b. In addition to the direct interactions discussed above there are numerous solvent-mediated hydrogen-bonding networks that link the functional groups of GSSG and GR.

Table 1

The interacting residues of $T[S]_2$ and TR.

$T[S]_2$ residue	Number of contacts A site	B site	Trypanothione-reductase residues
γGluI	10	24	Pro336, Ile339, Gly459′,His461′, Glu466′
CysI	8	5	Val54, Tyr111, Thr335, Ile339, His461′
GlyI	7	8	Ser15, Leu18, Tyr111, Ile339
Spm	18	14	Leu18, Glu19, Trp22, Ser110, Tyr111
γGluII	25	20	Val54, Val59, Lys62, Phe396, Lys399, His461′, Pro462′, Thr463′, Ser464′, Glu466′, Glu467′
CysII	5	5	Val59, Ile107, His461′
GlyII	1	0	Ile107

The number of contacts, excluding hydrogen bonds, with a distance restriction of 4.0 Å are listed; ′ signifies a residue from the partner subunit.

The determinants of specificity

TR and GR are mutually exclusive with respect to substrate specificity [10] and this has been ascribed to a combination of steric and electrostatic factors [8,14–17]. The substrates differ in size and charge but have conserved γ-glutamylcysteinyl moieties (Figure 1). GSSG is the smaller of the two and carries a net charge of –2 at physiological pH. $T[S]_2$ carries a net charge of +1 and a hydrophobic component of seven methylene groups on the Spm bridge.

Structural comparisons indicate differences in the orientation of domains with respect to each other, which influence the size of the GR and TR active sites [15–17]. Human GR has a smaller disulfide-substrate-binding site than TR. As a result, $T[S]_2$ is too large to fit optimally into the GR site and GSSG is too small to fit optimally into the TR active site. There are also specific amino acid alterations that affect both the size and the chemistry of the disulfide-substrate-binding sites. In human GR there are 19 amino acids implicated in the binding of GSSG, of which 14 are identical or homologous to residues in TR. These conserved residues include the catalytic machinery and, as one might expect, mainly interact with the γ-glutamylcysteinyl components of the substrates. The only significant difference involving this part of each substrate concerns γGluI. In the human GR–GSSG complex Arg347 interacts directly with γGluI. In *T. cruzi* TR this residue is replaced by Ala343, resulting in the loss of this electrostatic interaction and providing more freedom for the γGluI component of $T[S]_2$. There are five residues that interact with GSSG in human GR that are not conserved in TR: Ala34, Arg37, Ile113, Asn117 and Arg347 (Figure 4b). The corresponding residues in *T. cruzi* TR are Glu19, Trp22, Ser110, Met114 and Ala344 (Figure 4a); in addition, Arg38 in human GR is Asn23 in TR. The Arg347 to Ala344 difference has been discussed above. The locations of the remaining amino acid substitutions suggest that the substrate discrimination displayed by GR and TR is determined primarily on one side of their respective active sites. These substitutions change the narrow, positively charged and hydrophilic GR cleft into a wider TR active site with a hydrophobic patch adjacent to a negative glutamic acid. The positively charged human GR active site effectively binds the negatively charged GSSG but would repulse $T[S]_2$. The TR active site would repulse GSSG with a combination of charge repulsion and hydrophobic effects.

A protease-like catalytic triad and induced electronic fit

The disulfide oxidoreductases utilise an active-site histidine as the proton donor and acceptor in the catalytic cycle [7]. In *T. cruzi* TR this is His461. The imidazole is held in place with a hydrogen bond formed between Nδ1 and Oε1 of Glu466. Structures of human GR and *T. cruzi* TR, in the absence of substrate, have a solvent molecule positioned to bind to the active-site histidine Nε2 and the arrangement of functional groups in the Glu–His–Water assembly mimics that of a serine-protease catalytic triad [17]. When the substrate is bound, the CysI Sγ atom is positioned about 3 Å from Nε2 and optimally positioned to accept a relayed proton.

Investigation of catalytic-triad geometry in the serine proteases highlighted the role that a CH•••O hydrogen bond might play in fine tuning the chemical properties of the active-site histidine [18]. The specific interaction involves the His Cε1 with a mainchain carbonyl group that is always positioned to influence the catalytic histidine. In the TR–$T[S]_2$ complex we see a similar CH•••O interaction. However, the carbonyl-group hydrogen-bond acceptor is provided by the disulfide substrate and not, as observed in the proteases, by the protein mainchain. In the TR–$T[S]_2$ complex the distances between His461′ Cε1 and the γGluII carbonyl Oδ are 2.9 and 3.3 Å in active sites A and B, respectively. This interaction is also present in human GR when complexed with GSSG. Such an interaction, with the

Figure 5

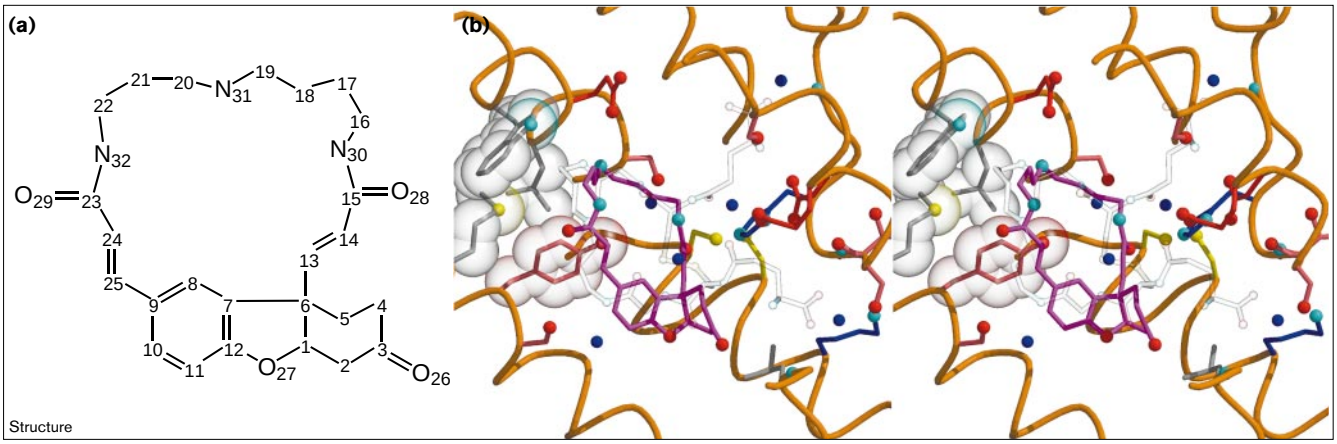

A novel inhibitor of trypanothione reductase. **(a)** Molecular formula of lunarine. **(b)** Stereoview showing a model of lunarine (magenta) in an active site of *T. cruzi* TR. For comparison, a 'ghostly' depiction of $T[S]_2$ is provided. The view and solvent positions are as in Figure 4a. This figure was produced using MOLSCRIPT [36].

resultant polarisation of the Cε1–H bond, may serve to stabilise the positive-charge distribution on the protonated histidine that is required for the catalytic function. TR and GR thus appear to be fine tuned for catalysis. Enzyme–ligand interactions position the substrates, which, in turn, prime the active-site base for catalysis. We term this electronic induced fit — the active centre is itself activated by the substrate it processes. This would contribute to the substrate specificity of TR and GR because each enzyme can only be optimally aligned for catalysis once the cognate substrate is in position. Such a structural feature may be an important consideration in the development of transition state analogue inhibitors of TR.

Structure-based inhibitor discovery

The molecular detail of the TR–$T[S]_2$ complex provides definition of the shape and electrostatic nature of the enzyme active site, the conformation of the substrate, details of the enzyme–ligand interactions and a structural explanation for the substrate discrimination displayed by TR and GR. This information is invaluable for structure-based identification of inhibitors. A difficulty with respect to TR is the size of both the active site and the substrate. $T[S]_2$ extends almost 17 Å in the longest dimension. To simplify the problem we concentrated on the interaction of the polyamine component of $T[S]_2$ with the hydrophobic patch and Glu19 of the TR active site I, which is where the major differences occur between TR and GR. The spermidine–carbonyl conjugate was used as a search fragment in the Cambridge Structural Database (CSD [19]) to identify a library of possible inhibitors. Two natural products, cadabacine (CSD entry FACWAH [20]) and lunarine (entry LUNARB10 [21]; Figure 5a) were selected for further investigation on the basis of several criteria. Firstly, these compounds have the spermidine moiety bound at either end by an amide group. This feature is shared with $T[S]_2$, and represents a key portion of the substrate with respect to TR specificity in addition to being an extension of the search template. Secondly, the molecules are cyclic and of comparable dimensions to $T[S]_2$, with a suitable electronic structure to impart some rigidity to the ring system. Thirdly, the size and chemistry of cadabacine and lunarine suggested that they would be unlikely to inhibit human GR.

Coordinates were retrieved from the CSD and positioned into the TR active site using the program DOCK 3.0 [22]. A shape descriptor of the active site was used to derive possible orientations of the molecules within it. The program GRID [23] was used to characterise the electrostatic properties of the TR cleft and this allowed us to identify and remove unfavourable orientations. The remaining arrangements of these molecules in the active site indicated a conserved placement of the spermidine components, enabling interaction with the hydrophobic patch, and a reasonable fit of the small molecules into the TR active site. We made no attempt to optimise or manipulate the fit of the molecules in the enzyme active site. One of the orientations of lunarine, selected arbitrarily, in the TR disulfide-substrate-binding cleft is presented in Figure 5b. The modelling suggested that these natural products could be selective inhibitors of TR and we sought to validate this hypothesis experimentally. Although unable to obtain a sample of cadabacine, we did obtain lunarine and characterised its inhibition kinetics against *T. cruzi* TR and human GR. Lunarine was found to be a selective inhibitor of TR; human GR was not significantly inhibited by 500 μM lunarine under conditions that inhibit TR by 97%. This result confirmed our predictions. Unexpectedly, the inhibition pattern does not conform to that of a simple competitive inhibitor in that it shows time dependence involving

Figure 6

Inhibition of trypanothione reductase by lunarine. **(a)** Residual activity as a function of lunarine concentration: no drug (triangles); plus drug: 62.5 μM, (open circles); 125 μM, (closed circles); 250 μM, (open squares); 500 μM, (closed squares). **(b)** Observed rate of inactivation as a function of lunarine concentration. Bars indicate the standard error for each data set.

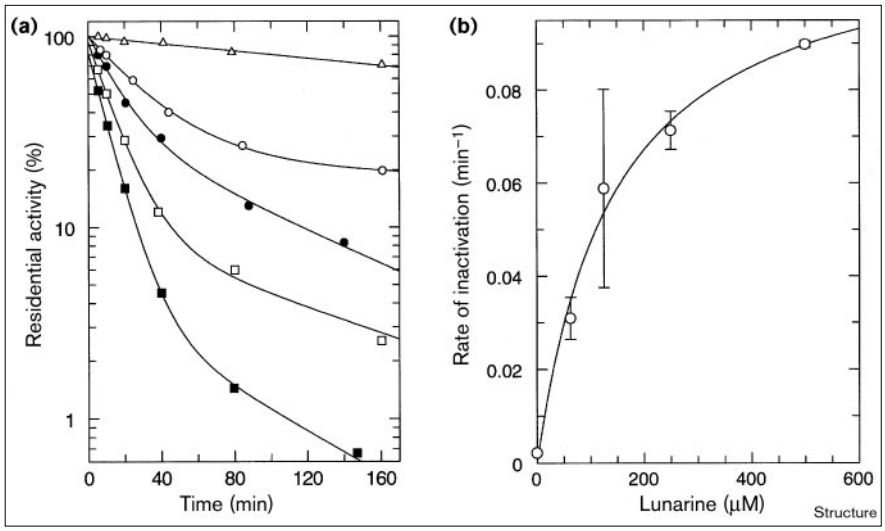

the NADPH-reduced (EH_2) form of the enzyme. Inhibition is both time- and concentration-dependent and can be fitted to a double exponential decay equation (Figure 6). Within experimental error, the rate constant for the second phase approximates the rate of inactivation by NADPH in the absence of lunarine. In contrast, the rate constant for the first phase is hyperbolic with respect to inhibitor concentration from which an apparent K_i of 144 ± 30.5 μM and k_{inact} of 0.116 ± 0.009 min^{-1} can be derived. We conclude that inhibition most likely involves a reversible multi-step mechanism of the type:

$$E + I \Leftrightarrow EI \Leftrightarrow E^*I$$

where EI represents a non-covalent Michaelis-type enzyme inhibitor intermediate complex and E*I a subsequent covalent complex between lunarine and the two electron-reduced form of TR. This mode of inhibition of TR has been observed before, in particular with arsenical drugs that are in clinical use [24]. The modest K_i of 144 μM for lunarine is encouraging when compared to a binding constant of approximately 40 μM for $T[S]_2$ and allows considerable scope for improvement. A useful lead compound should be amenable to chemical modification and inspection of the lunarine structure (Figure 5a) indicates at least two positions where nucleophilic attack (Michael addition) can occur to permit synthetic modifications of the molecular framework. We had not predicted the possibility of a covalent link between lunarine and the reduced form of TR in advance of the kinetic studies. The observation provides further support for the use of these alkaloids as lead compounds and even suggests that components of lunarine might be suitable for the development of suicide inhibitors of a range of disulfide oxidoreductases. If, as is likely, Michael addition has occurred between lunarine and TR, and the model presented in Figure 5b is correct, then addition at C13 would be favoured over C25.

Concluding remarks

An important aspect of the pharmaceutical industries' research effort is the hunt for naturally occurring molecules with biological activity. This is based on the historical lesson that many therapeutic agents are natural products, or derivatives thereof, identified in part on the basis of folk lore. Important examples are quinine from Chinchona bark and artemesinin from Chinese herbal extracts [3]. Both of these compounds are used for the treatment of malaria, which is a serious protozoan-parasite infection. Our search for new inhibitors of TR has identified two alkaloids extracted from plants that are also used in folk medicine [e.g. 25]. Cadabacine is derived from a shrub (*Cadaba farinosa*) grown throughout South and Eastern Africa, the Middle East and Asia. Lunarine is derived from the common European garden plants *Lunaria biennis* and *L. rediviva*. Lunarine has been confirmed as a novel inhibitor of *T. cruzi* TR and this family of natural products now provides a series of promising lead compounds for further experiments designed to improve inhibition properties in the search for a molecule of medicinal value.

Biological implications

Several species of protozoa of the order Kinetoplastida, suborder Trypanosomatina, are the causal agents of a variety of serious tropical diseases afflicting humans and livestock. New and improved anti-trypanosomal drugs are urgently sought because current therapies are inadequate as a result of the low efficacy and high toxicity of available drugs. Vaccines have not been forthcoming and the problem is compounded by the ability of the parasites to develop drug resistance.

The enzyme trypanothione reductase (TR) is unique to the Trypanosomatina, where it is a key component of the parasites' antioxidant defence systems. TR has been validated as a target for the development of new anti-trypanosmal drugs by molecular genetics methods. As a component of a structure-based approach to drug identification, we have characterised the three-dimensional structure of TR from one of the most important human parasites, *Trypanosoma cruzi*, in complex with one of the physiological substrates, trypanothione. The complex provides structural detail that explains enzyme specificity and characterises the binding site for the disulfide substrate in terms of van der Waals interactions, and hydrogen-bond donors and acceptors. The substrate provides templates for searching chemical libraries in an attempt to find molecules able to bind in the active site and function as inhibitors. The enzyme active site provides a target for characterisation using computational methods that suggest the electrostatic and steric criteria that prospective ligands must fulfil. Our utilisation of the model in database searches and molecular modelling has identified the polyamine-bearing alkaloids, cadabacine and lunarine, as candidates for inhibition trials. Lunarine has been confirmed as a selective inhibitor of *T. cruzi* TR, but it essentially has no effect on the homologous human enzyme, glutathione reductase. These natural products now provide a series of lead compounds for further experiments designed to improve inhibition properties in the search for a molecule of medicinal value.

Materials and methods

Purification, crystallization and data collection

Recombinant enzymes were purified from *E. coli* using methods previously described [26]. Trypanothione was purchased from Bachem, Germany. Co-crystallization of TR and $T[S]_2$ was achieved using conditions previously reported [27]. The best crystals were obtained when a ratio of monomer:substrate of approximately 1:0.9 was used. Yellow rods in space group $P4_3$, with $a = b = 93.33$, $c = 157.14$ Å grew in several days. These crystals are isomorphous with the native structure and contain a homodimer in the asymmetric unit. Diffraction data were recorded at 4°C from a crystal of dimensions $0.2 \times 0.2 \times 1.1$ mm, mounted in a capillary with mother liquor, on station PX9.6 (λ 0.92 Å / Mar Research image plate) at the Synchrotron Radiation Source at Daresbury Laboratory. Data were processed using the MOSFLM [28] and CCP4 programs [29]. The data comprised 142,903 I σ(I) measurements of 45,818 unique reflections (R_{sym} 7.5%) to a resolution of 2.4 Å. This represents 87.4% coverage.

Structure refinement

The starting model was the native *T. cruzi* TR structure [17]. Refinement was carried out with the program X-PLOR [30] using the Engh and Huber dictionary for restraints [31] and similar protocols as those employed in the native structure. Map calculations used CCP4 programs [29], computer graphics checking and analysis used FRODO [32] and O [33]. The stereochemical quality of the model was monitored with PROCHECK [34]. At an early stage of the analysis we observed distinct conformations for γGlul. In one active site (A) there are a number of solvent-mediated contacts to residues on the interface domain; in the other active site γGlul is more buried, forms an increased number of van der Waals interactions with the enzyme and participates in hydrogen bonds to both mainchain and sidechain atoms of the interface domain. The substrate was gradually built into difference maps during the refinement, incorporated into the calculations and checked with the use of omit maps. Solvent positions were treated as oxygens and checked after each round of refinement. Solvents in the disulfide-substrate-binding site were only included in refinement when the substrate had been completely modelled.

Refinement converged with an R factor of 20.9% for 41,129 reflections with $F > \sigma F$ in the range 8.0–2.4 Å resolution. The final model comprises residues 2–486 of subunit A, 9–486 of subunit B (7459 non-hydrogen atoms), two FAD molecules (106 atoms), 409 waters and two molecules of $T[S]_2$ (96 atoms). The model has rms deviations in bond lengths, bond angles, dihedral and improper angles of 0.011 Å, 2.7°, 24.5° and 1.8°, respectively. Average thermal parameters are 29.4 and 35.7 $Å^2$ for all protein atoms of subunits A and B, respectively; 15.3 and 25.0 $Å^2$ for the FAD groups; 73.5 and 73.1 $Å^2$ for substrate in binding sites A and B. Solvent molecules have an average thermal parameter of 47.5 $Å^2$. The substrate disulfide electron density in omit maps has been compared to the enzyme disulfide peak heights and suggests an occupancy of approximately 0.5 for the substrate. We maintained unit occupancy of the substrate atoms and let the thermal parameters account for any lower value. Nuclear magnetic resonance spectroscopy indicates that $T[S]_2$ displays a considerable degree of conformational flexibility [35]. We suggest that a combination of partial occupancy and flexibility explains the observed thermal parameters. A Ramachandran plot [34] has 90.8% of residues in most favoured regions and a further 8.6% in allowed regions. Five residues are in disallowed regions: Lys4A, Lys305A, Ala263B, Phe45A and Phe45B. The phenylalanines are in well-defined loops with the mainchains held in a strained conformation.

Inhibitor studies

Enzymes were stored as suspensions in ammonium sulphate and dialysed against assay buffer before use. TR (3 nM) was assayed using a Beckman DU640 spectrophotometer in 40 mM (K^+) HEPES, pH 7.5, 1 mM EDTA and 0.27 mM NADPH in a total volume of 0.5 ml at 26°C, followed by the addition of $T[S]_2$ (0.1 mM). GR (24 nM) was assayed in a similar manner, but in 40 mM (K^+) HEPES, pH 7.0, 1 mM EDTA, 80 mM KCl and 0.27 mM NADPH followed by the addition of 0.1 mM GSSG. Enzyme mixtures were preincubated with NADPH (5 min at 26°C) before the addition of varying concentrations of lunarine (stock solution 12.5 mM in dimethylsulphoxide). At varying times following the addition of inhibitor the reaction was initiated by the addition of the appropriate substrate. As a result of the interfering absorbance of lunarine at 340 nm, oxidation of NADPH was monitored at 366 nm using an extinction coefficient of 3300 M^{-1} cm^{-1} and all experiments were performed in triplicate.

Accession numbers

Structure factors and coordinates have been deposited in the PDB and assigned accession numbers R1BZLSF and 1BZL, respectively.

Acknowledgements

The work was funded by the Wellcome Trust, an Overseas Research Scholarship to YZ, BBSRC/EPSRC and the Daresbury Synchrotron Laboratory. We acknowledge the EPSRC-funded Chemical Database Service at Daresbury. We thank C Poupat for the gift of lunarine, S Bailey and R Nuttall for discussions, S McSweeney and P Rizkallah for support at Daresbury and referees for constructive criticisms.

References

1. Moncayo, A. (1993). Chagas' disease. In *Tropical Disease Research; Progress 1991-92*, pp. 67-76. World Health Organisation, Geneva.
2. de Castro, S. (1993). The challenge of Chagas' disease chemotherapy: an update of drugs assayed against *Trypanosoma cruzi. Acta Trop.* **53**, 83-98.
3. Schirmer, R.H., Muller, J.G. & Krauth-Siegel, R.L. (1995). Disulfide-reductase inhibitors as chemotherapeutic agents: the design of drugs for trypanosomiasis and malaria. *Angew. Chem. Int. Ed. Engl.* **34**, 141-154.

4. Verlinde, C.L.M.J. & Hol, W.G.J. (1994). Structure-based drug design: progress, results and challenges. *Structure* **2**, 577-587.
5. Marton, L.J. & Pegg, A.E. (1995). Polyamines as targets for therapeutic intervention. *Annu. Rev. Pharmacol. Toxicol.* **35**, 55-91.
6. Dolphin, D., Poulson, R. & Avramovic, O. (1989). *Glutathione; Chemical, Biochemical and Medical Aspects*. John Wiley & Sons, New York, USA.
7. Karplus, P.A. & Schulz, G.E. (1989). Substrate binding and catalysis by glutathione reductase as derived from refined enzyme:substrate crystal structures at 2.0 Å resolution. *J. Mol. Biol.* **210**, 163-180.
8. Fairlamb, A.H. & Cerami, A. (1992). Metabolism and functions of trypanothione in the kinetoplastida. *Annu. Rev. Microbiol.* **46**, 695-729.
9. Henderson, G.B., Fairlamb, A.H., Ulrich, P. & Cerami, A. (1987). Substrate specificity of the flavoprotein trypanothione disulfide reductase from *Crithidia fasciculata*. *Biochemistry* **26**, 3023-3027.
10. Dumas, C., *et al*., & Papadopoulou, B. (1997). Disruption of the trypanothione reductase gene of *Leishmania* decreases its ability to survive oxidative stress in macrophages. *EMBO. J.* **16**, 2590-2598.
11. Tovar, J., Cunningham, M.L., Smith, A.C., Croft, S.L. & Fairlamb, A.H. (1998). Down-regulation of *Leishmania donovani* trypanothione reductase by heterologous expression of a trans-dominant mutant homologue: effect on parasite intracellular survival. *Proc. Natl Acad. Sci. USA* **95**, 5311-5316.
12. Tovar, J., Wilkinson, S., Mottram, J.C. & Fairlamb, A.H. (1998) Evidence that trypanothione reductase is an essential enzyme in Leishamania by targeted replacement of the *tryA* gene locus. *Mol. Microbiol.* **29**, 653-660.
13. Stoll, V.S., Simpson, S.J., Krauth-Siegel, R.L., Walsh, C.T. & Pai, E.F. (1997). Glutathione reductase turned into trypanothione reductase: structural analysis of an engineered change in substrate specificity. *Biochemistry* **36**, 6437-6447.
14. Bailey, S., Smith, K., Fairlamb, A.H. & Hunter, W.N. (1993). Substrate interactions between trypanothione reductase and N^1-glutathionylspermidine disulfide at 0.28nm resolution. *Eur. J. Biochem.* **213**, 67-75.
15. Kuriyan, J., *et al*., & Henderson, G.B. (1991). X-ray structure of trypanothione reductase from *Crithidia fasciculata* at 2.4 Å resolution. *Proc. Natl Acad. Sci. USA* **88**, 8764-8768.
16. Hunter, W.N., *et al*., & Fairlamb, A.H. (1992). Active site of trypanothione reductase; a target for rational drug design. *J. Mol. Biol.* **227**, 322-333.
17. Zhang, Y., Bond, C.S., Bailey, S., Cunningham, M.L., Fairlamb, A.H. & Hunter, W.N. (1996). The crystal structure of trypanothione reductase from the human pathogen *Trypanosoma cruzi* at 2.3 Å resolution. *Protein Sci.* **5**, 52-61.
18. Derewenda, Z.S., Derewenda, U. & Kobos, P.M. (1994). His Cε-H···O=C< hydrogen bond in the active site of serine hydrolases. *J. Mol. Biol.* **241**, 83-93.
19. Allen, F.H. & Kennard, O. (1993). 3D search and research using the Cambridge Structural Database. *Chem. Design. Auto. News*. **8** , 130-137.
20. Ahmed, V.U., Amber, A., Arif, S., Chen, M.H.M. & Clardy, J. (1985). Cadabacine, an alkaloid from *Cadaba farinosa*. *Phytochemistry*. **24**, 2709-2711.
21. Tamura, C. & Sim, G.A. (1970). Molecular conformations. Part X. A skew boat cyclohexanone: X-ray analysis of lunarine hydrobromide hydrate. *J. Chem. Soc.* (B) 991-995.
22. Kuntz, I.D. (1992). Structure-based strategies for drug design and discovery. *Science* **257**, 1078-1082.
23. Goodford, P.J. (1985). A computational procedure for determining energetically favorable binding sites on biologically important macromolecules. *J. Med. Chem.* **28**, 849-857.
24. Cunningham, M.L., Zvelebil, M.J.J.M. & Fairlamb, A.H. (1994). Mechanism of inhibition of trypanothione reductase and glutathione reductase by trivalent organic arsenicals. *Eur. J. Biochem.* **221**, 285-295.
25. Breyer-Brandwijk, M.G. & Watt, J.M. (1962). *The Medicinal and Poisonous Plants of Southern and Eastern Africa*. (2nd edn), E. & S. Livingston Ltd, Edinburgh, UK.
26. Borges, A., Cunningham, M.L., Tovar, J. & Fairlamb, A.H. (1995). Site-directed mutagenesis of the redox-active cysteines of *Trypanosoma cruzi* trypanothione reductase. *Eur. J . Biochem.* **228**, 745-752.
27. Zhang, Y., *et al*., & Hunter, W.N. (1993). *Trypanosoma cruzi* trypanothione reductase, crystallization, unit cell dimensions and structure solution. *J .Mol. Biol.* **233**, 1217-1220.
28. Leslie, A.G.W. (1993). Joint CCP4 and ESF-EACMB Newsletter on Protein Crystallography. Daresbury Laboratory, Warrington, UK.
29. Collaborative Computational Project Number 4. (1994). The CCP4 suite: programs for protein crystallography. *Acta Cryst. D* **50**, 760-763.
30. Brünger, A.T. (1990). X-PLOR (V 2.2) Manual. Howard Hughes Medical Institute, Yale University.
31. Engh, R.A. & Huber, R. (1991). Accurate bond and angle parameters for X-ray protein-structure refinement. *Acta Cryst. A* **47**, 392-400.
32. Jones, T.A. (1985). FRODO-A graphic model building and refinement system for macromolecules. *Methods Enzymol.* **115**, 157-171.
33. Jones, T.A., Zou, J.Y., Cowan, S.W. & Kjeldgaard, M. (1991). Methods for building protein models in electron density maps and the location of errors in these models. *Acta Cryst. A* **47**, 110-119.
34. Laskowski, R.A., MacArthur, M.W., Moss, D.S. & Thornton, J.M. (1993). PROCHECK: a program to check the stereochemical quality of protein structures. *J. Appl. Cryst.* **26**, 283-291.
35. Henderson, G.B., Glushka, J., Cowburn, D. & Cerami, A. (1990). Synthesis and NMR characterisation of the trypanosomatid metabolite, N^1, N^8-*bis*(glutathionyl)spermidine disulfide (trypanothione disulfide). *J. Chem. Soc. Perkin Trans*. **1**, 911-914.
36. Kraulis, P.J. (1991). MOLSCRIPT: a program to produce both detailed and schematic plots of protein structures. *J. Appl. Cryst.* **24**, 946-950.
37. Merritt, E.A. & Murphy, M.E.P. (1994). Raster3d, a program for photorealistic molecular graphics. *Acta Cryst. D* **50**, 869-873.

Because *Structure with Folding & Design* operates a 'Continuous Publication System' for Research Papers, this paper has been published on the internet before being printed (accessed from http://biomednet.com/cbiology/str). For further information, see the explanation on the contents page.